Ultra-small shape-simplified optical diode derived from topology optimal design in plasmonic waveguide

doi: info:doi/10.1587/elex.16.20190598

IEICE Electronics Express, Vol.16, No.22, 1–4

LETTER

Ultra-small shape-simplified optical diode derived from topology optimal design in plasmonic waveguide

Akito Iguchi[1,2] **and Yasuhide Tsuji**[1a)]

Abstract We present in this paper an ultra-small plasmonic optical diode, which converts a symmetric mode into an asymmetric one and reflects backward propagation of the symmetric one, with a metal-insulator-metal (MIM) structure. A profile of an optical diode is derived from a topology optimal structure obtained in our previous study, and it is simplified so as to reduce insertion loss and difficulty in fabrication. An optimal profile is found out using a differential evolution (DE) which is one of the evolutionary algorithms, and optimization is carried out taken into account fabrication tolerance. According to the results of numerical simulation by 2D finite element method (FEM), the optimized plasmonic optical diode has insertion loss of <0.5 dB, reflection of <−20 dB in the forward propagation, and backward transmission of <−20 dB over C-band, and it is tolerant of ±5 nm boundary deviation. In addition, this device has an extremely small functional region (<1.5 μm).

Keywords: optical waveguide, optical diode, plasmonics, evolutionary algorithms

Classification: Integrated optoelectronics

1. Introduction

Recently, more-compact and high-performance optical waveguide devices are required so as to realize higher density photonic integrated circuits for higher-speed optical communication networks. Among optical components, an optical diode is perceived as one of the key and attractive components for optical integrated circuits [1]. An optical diode can offer an unidirectional building block only using reciprocal materials [1, 9, 10], and a lot of studies on an optical diode have already been reported [1, 2, 3, 4, 5, 6, 7, 8]. As a solution for miniaturization, optical diode based on photonic crystal (PhC) waveguide are presented [5, 6, 7]. This type of optical diodes achieve extremely small footprint, but there is room for improvement especially in an operation wavelength range. A plasmonic waveguide is also a good candidate to realize high-integration of optical circuits because it can confine light to waveguide regions beyond diffraction limits [11]. So far, miniaturization has been achieved for many optical components by using plasmonic effects [12, 13, 14, 15, 16, 17, 18, 19, 20, 21].

Structural optimization utilizing numerical simulation is widely employed to design photonic devices. Topology optimization is one of the structural optimization methods and has the highest design of freedom. It has been applied to a design of optical components composed of dielectric materials [22, 23, 24, 25, 26, 27]. In [28], The author's group present a design approach with topology optimization for plasmonic waveguide devices. In the previous work, using topology optimization based on a function expansion method and evolutional algorithms, an extremely small plasmonic optical diode is designed with a metal-insulator-metal (MIM) structure. However, the topology optimal diode has complex profiles which induce localization of lightwave, and this localization causes extra propagation loss because of lossy nature of metal materials. Moreover, a simpler profile is desirable in terms of actual fabrication.

In this paper, we present an ultra-small, shape-simplified plasmonic optical diode which is derived from topology optimal structure reported in [28]. Extracting geometrical features from the topology optimal one, we offer an optical diode with simpler profile. The optical diode consists of two triangular objects and a rectangular one. The vertex coordinates of these objects are optimized using a differential evolution (DE) [29] which is one of the evolutionary algorithms. Moreover, in the DE optimization, fabrication tolerance of material boundary deviation is newly taken into account.

2. Optical diode and design methods

A function of an ideal optical diode is shown in Fig. 1. An optical diode converts completely a symmetric mode into an asymmetric one for forward input, and reflects backward wave of the symmetric one. Although unidirectional operation can be achieved only using reciprocal materials, it is pointed out that its scattering matrix is symmetry and reciprocity holds [1, 9, 10]. In this study, we consider an plasmonic optical diode which transforms from a funda-

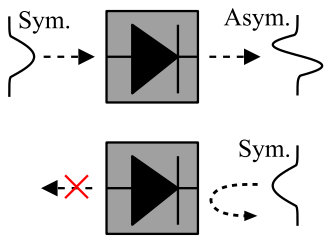

Fig. 1. A function of an ideal optical diode.

[1]Division of Information and Electronic Engineering, Muroran Institute of Technology, 27–1 Mizumoto-cho, Hokkaido 050–8585, Japan
[2]Research Fellow of Japanese Society for the Promotion of Science
a) y-tsuji@mmm.muroran-it.ac.jp

DOI: 10.1587/elex.16.20190598
Received September 24, 2019
Accepted October 28, 2019
Publicized November 11, 2019
Copyedited November 25, 2019

Fig. 2. Topology optimal plasmonic optical diode given in [28]. Black color indicates silver and white means air.

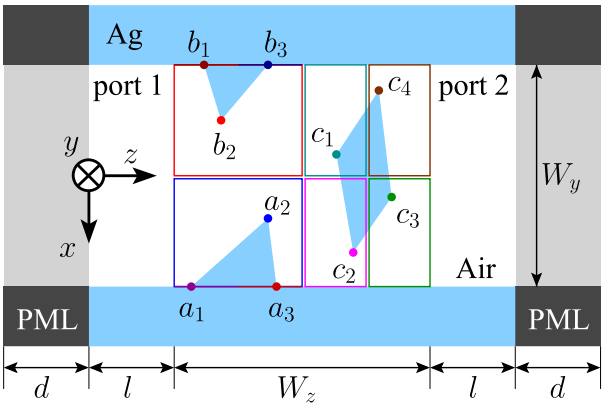

Fig. 3. The schematic of a plasmonic optical diode. The computational window in z-direction is terminated by perfectly matched layer (PML).

Table I. Constraint condition of 10 vertex coordinates.

a_1:	$0.5\,\mu\text{m} \le a_{1z} \le 1\,\mu\text{m}$,	$a_{1x} = -0.4\,\mu\text{m}$
a_2:	$0.5\,\mu\text{m} \le a_{2z} \le 1.5\,\mu\text{m}$,	$-0.39\,\mu\text{m} \le a_{2x} \le -0.01\,\mu\text{m}$
a_3:	$1.01\,\mu\text{m} \le a_{3z} \le 1.5\,\mu\text{m}$,	$a_{3x} = -0.4\,\mu\text{m}$
b_1:	$0.5\,\mu\text{m} \le b_{1z} \le 1\,\mu\text{m}$,	$b_{1x} = 0.4\,\mu\text{m}$
b_2:	$0.5\,\mu\text{m} \le b_{2z} \le 1.5\,\mu\text{m}$,	$0.01\,\mu\text{m} \le b_{2x} \le 0.39\,\mu\text{m}$
b_3:	$1.01\,\mu\text{m} \le b_{3z} \le 1.5\,\mu\text{m}$,	$b_{3x} = 0.4\,\mu\text{m}$
c_1:	$1.51\,\mu\text{m} \le c_{1z} \le 1.75\,\mu\text{m}$,	$-0.39\,\mu\text{m} \le c_{1x} \le 0.01\,\mu\text{m}$
c_2:	$1.51\,\mu\text{m} \le c_{2z} \le 1.75\,\mu\text{m}$,	$0.01\,\mu\text{m} \le c_{2x} \le 0.39\,\mu\text{m}$
c_3:	$1.76\,\mu\text{m} \le c_{3z} \le 2\,\mu\text{m}$,	$0.01\,\mu\text{m} \le c_{3x} \le 0.39\,\mu\text{m}$
c_4:	$1.76\,\mu\text{m} \le c_{4z} \le 2\,\mu\text{m}$,	$-0.39\,\mu\text{m} \le c_{4x} \le -0.01\,\mu\text{m}$

mental TM wave (TM_0) into TM_1 wave in the forward direction, and shuts off backward transmission of these waves.

Fig. 2 shows the plasmonic optical diode obtained by topology optimization in [28]. The profile can be interpreted as a device composed of two triangular objects and a rectangular island. The solid red line is a simplified profile of an optical diode studied in this paper. A design schematic in the plasmonic optical diode is shown in Fig. 3. The dimensions shown in the figure are as follows: $l = 0.5\,\mu\text{m}$, $W_y = 0.8\,\mu\text{m}$, $W_z = 1.5\,\mu\text{m}$. A computational window in z-direction is terminated by a perfectly matched layer (PML) with thickness of $d = 0.5\,\mu\text{m}$. The permittivity of silver (Ag) is determined by a Lorentz-Drude model presented in [30], and the relative permittivity of air is 1. We estimate a propagating field and output power using 2D finite element method (FEM) [31].

We solve the minimization problem of the following objective function to optimize the simplified optical diode:

$$\text{minimize } f = \sum_{\Delta\in\{-5\,\text{nm},0\,\text{nm},+5\,\text{nm}\}} (f_1 + f_2 + f_3) \quad (1)$$

with

$$f_1 = (1 - |S_{21}^{(0\to1)}|^2)^2$$
$$f_2 = \alpha(0 - |S_{11}^{(0\to0)}|^2)^2$$
$$f_3 = \beta(0 - |S_{12}^{(0\to0)}|^2 - |S_{12}^{(0\to1)}|^2)^2$$

where superscripts of S-parameters denotes mode order of input and output TM waves. These S-parameters are estimated at the wavelength of 1.55 µm. f_1 is a term to achieve TM_0-to-TM_1 conversion, and f_2 is one to reduce reflection in forward propagation. By minimizing f_3, backward transmission is shut off. Δ denotes deviation of material boundary. In this study, we design an optical diode to be tolerant of ±5 nm over- and under-etching. α and β are weight factors, and they are let $\alpha = \beta = 10^2$ so that low reflection in the forward input and high backward rejection are achieved. We optimize 10 vertex coordinates of the extracted objects using the DE [29]. To avoid collision between the objects, we restrict movable region of the vertexes as Table I. x-positions of vertexes, a_{1x}, a_{3x}, b_{1x}, and b_{3x}, are fix not to break the original profile.

In the DE algorithm, first, the design parameter vector is randomly generated N_p times. Then, mutant vector, $\{v\}'_i$ ($i \in [0, N_p - 1]$), is created at random according to crossover ratio, C_r, as follows:

$$\{v\}'_i = \{v\}_i + F(\{v\}_{p1} - \{v\}_{p2}) \quad (2)$$

where F is a scale factor, $\{v\}_{p1}$ and $\{v\}_{p2}$ are randomly selected vectors ($p1, p2 \in [0, N_p - 1]$). If a mutant vector has greater potential, a previous vector is discarded and is replaced by the mutant vector. We iterate the mutation and the replacing procedure 200 times with DE parameters of $N_p = 120$, $C_r = 50\%$, and $F = 0.5$.

3. Optimization results

Fig. 4 shows the value of the objective function as a function of DE iteration number. Since the DE is based on a random searching algorithm, we conduct 10 optimization runs with the same DE parameters. It takes about 2 hours to finish 1 DE optimization run using a workstation with Intel Xeon CPU X5690@3.47 GHz. As shown in the figure, the values converge around $f = 2 \times 10^{-2}$, and the smallest value is 1.78×10^{-2}. The optimized profile and propagation waves are shown in Fig. 5. Optimized vertex coordinates

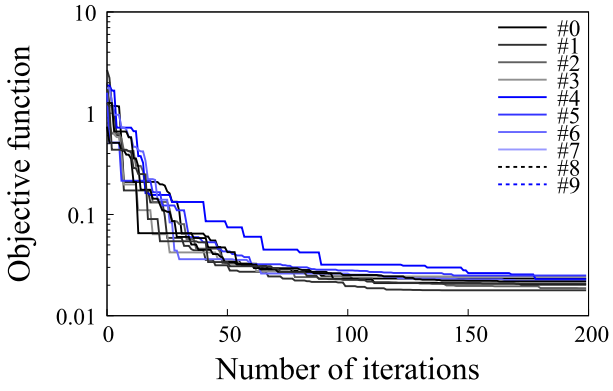

Fig. 4. The value of objective function as a function of iteration number in 10 DE optimization runs.

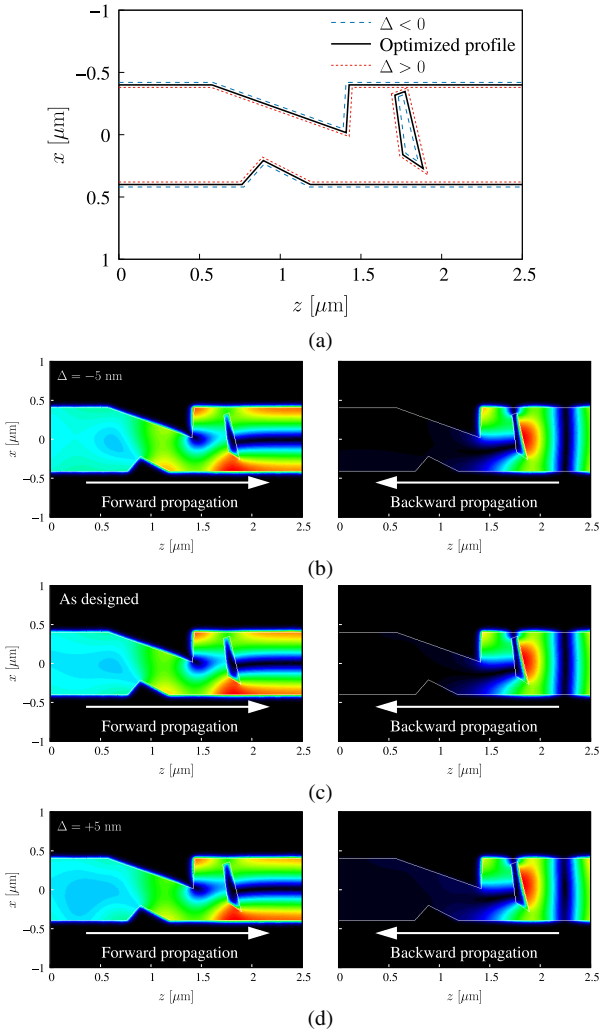

Fig. 5. Optimized profile of a plasmonic optical diode and propagation fields in the optimized plasmonic diode. (a) The optimized profile of the simplified optical diode. (b), (c), and (d) are propagation fields at wavelength of 1.55 μm when boundary deviation, Δ, is (b) −5 nm, (c) 0 nm, and (d) +5 nm.

are listed in Table II. Fig. 5(b), (c), and (d) are propagating waves at wavelength of 1.55 μm. We can see that TM_0-to-TM_1 conversion in the forward propagation and rejection of the backward propagation, that is, the functions of an optical diode are achieved in the optimized structure. Moreover, the diode functions are maintained even if ±5 nm boundary deviation is caused. Transmittance and reflectance spectra in the optimized optical diode are given in Fig. 6. We define the transmittance and reflectance as follows:

$$\text{Transmit.(forward)} = 10\log_{10}(|S_{21}^{(0\to1)}|^2)$$

$$\text{Reflect.(forward)} = 10\log_{10}(|S_{11}^{(0\to0)}|^2 + |S_{11}^{(0\to1)}|^2)$$

$$\text{Transmit.(backward)} = 10\log_{10}(|S_{12}^{(0\to0)}|^2 + |S_{12}^{(0\to1)}|^2).$$

Fig. 6(a) is transmission spectra of TM_1 wave transformed from TM_0 wave in the forward propagation, and Fig. 6(b) shows reflection spectra observed at port 1. The optimized optical diode has insertion loss of less than 0.5 dB for ±5 nm boundary deviation in the wide wavelength range from 1469 nm to 1624 nm. Reflection is less than −20 dB over the range from 1511 nm to 1585 nm covering C-band. These results shows that under-etching induce red-shift in transmittance and reflectance spectra. A resonant cavity is made of the rectangular island and the larger triangular object, and this shift may be attributed to the change of resonant frequency of the cavity. Backward transmittance spectra are shown in Fig. 6(c). For the ±5 nm variation, backward

Table II. Optimized vertex coordinates of the feature objects with the DE.

a_1:	$a_{1z} = 0.763342\,\mu m$,	$a_{1x} = 0.4\,\mu m$
a_2:	$a_{2z} = 0.895082\,\mu m$,	$a_{2x} = 0.207506\,\mu m$
a_3:	$a_{3z} = 1.186733\,\mu m$,	$a_{3x} = 0.4\,\mu m$
b_1:	$b_{1z} = 0.576922\,\mu m$,	$b_{1x} = -0.4\,\mu m$
b_2:	$b_{2z} = 1.408439\,\mu m$,	$b_{2x} = -0.016381\,\mu m$
b_3:	$b_{3z} = 1.426864\,\mu m$,	$b_{3x} = -0.4\,\mu m$
c_1:	$c_{1z} = 1.710309\,\mu m$,	$c_{1x} = -0.317124\,\mu m$
c_2:	$c_{2z} = 1.759773\,\mu m$,	$c_{2x} = 0.160880\,\mu m$
c_3:	$c_{3z} = 1.885142\,\mu m$,	$c_{3x} = 0.270315\,\mu m$
c_4:	$c_{4z} = 1.773301\,\mu m$,	$c_{4x} = -0.347117\,\mu m$

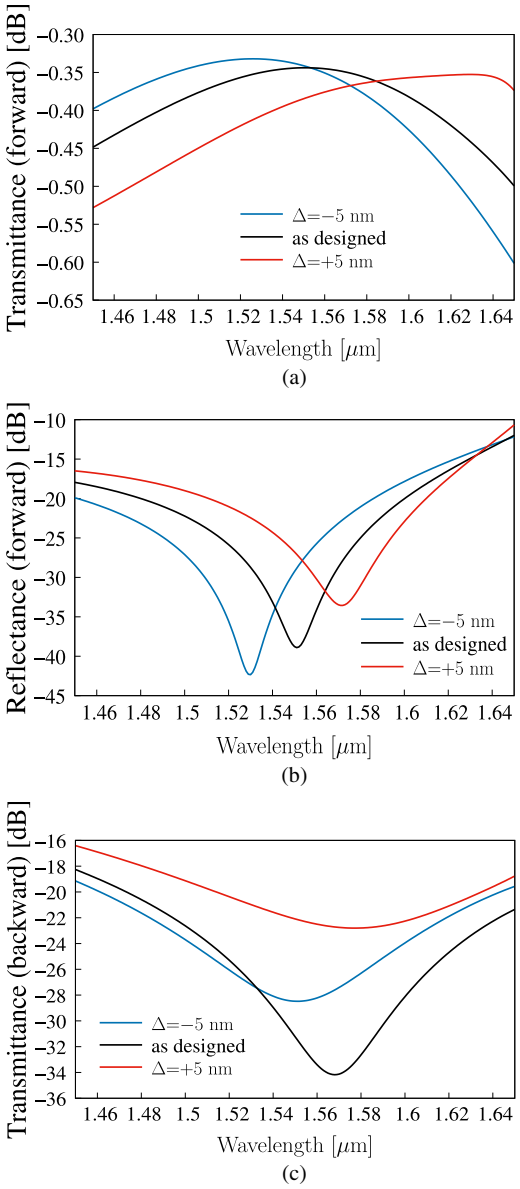

Fig. 6. Transmittance and reflectance spectra in the optimized plasmonic optical diode. (a) Transmittance of a converted TM_1 wave at port 2, (b) Reflectance at port 1 in the forward propagation, and (c) Backward transmittance at port 1.

transmission is less than −20 dB over the range from 1515 nm to 1634 nm. The functional region is extremely small in the longitudinal direction (<1.5 μm), and this optical diode achieve insertion loss of <0.5 dB, reflection of <−20 dB, and backward transmission of <−20 dB over C-band for ±5 nm over- and under-etching. It has lower-loss than topology optimal optical diode shown in the previous paper [28]. This is because unnecessary complex structure which induces localization of lightwave is avoided by simplification of a profile.

4. Conclusion

We presented a shape-simplified, ultra-small plasmonic optical diode which is derived from a topology optimal profile. A simplified profile was optimized by the DE algorithm, and we found out the plasmonic optical diode which has insertion loss of <0.5 dB, reflection of <−20 dB, and backward transmission of <−20 dB over the range from 1515 nm to 1585 nm covering C-band for ±5 nm boundary deviation. By the simplification approach, a lower-loss plasmonic optical diode was obtained compared to the topology optimized one.

Topology optimization offers attractive and novel profiles, but it is difficult to obtain a simple profile which has sufficient performance because of its design of freedom. The design procedure conducted in this paper can be applied to the other optical components. If the simplification procedure is automated, this design procedure becomes more useful, and it is our future works.

Acknowledgments

This work is partially supported by JSPS KAKENHI Grant Number JP 19J14709, and the authors would like to thank fundamental studies by Y. Nagata.

References

[1] V. Liu, *et al.*: "Ultra-compact photonic crystal waveguide spatial mode converter and its connection to the optical diode effect," Opt. Express **20** (2012) 28388 (DOI: 10.1364/OE.20.028388).
[2] L. Feng, *et al.*: "Nonreciprocal light propagation in a silicon photonic circuit," Science **333** (2011) 729 (DOI: 10.1126/science.1206038).
[3] C. Wang, *et al.*: "On-chip optical diode based on silicon photonic crystal heterojunctions," Opt. Express **19** (2011) 26948 (DOI: 10.1364/OE.19.026948).
[4] C. Lu, *et al.*: "Ultrahigh-contrast and wideband nanoscale photonic crystal all-optical diode," Opt. Lett. **36** (2011) 4668 (DOI: 10.1364/OL.36.004668).
[5] S. Feng, *et al.*: "Unidirectional reciprocal wavelength filters based on the square-lattice photonic crystal structures with the rectangular defects," Opt. Express **21** (2013) 220 (DOI: 10.1364/OE.21.000220).
[6] H. Ye, *et al.*: "Ultra-compact broadband mode converter and optical diode based on linear rod-type photonic crystal waveguide," Opt. Express **23** (2015) 9673 (DOI: 10.1364/OE.23.009673).
[7] H. Ye, *et al.*: "Realization of compact broadband optical diode in linear air-hole photonic crystal waveguide," Opt. Express **24** (2016) 24592 (DOI: 10.1364/OE.24.024592).
[8] J. Li, *et al.*: "Design of a broadband reciprocal optical diode in a silicon waveguide assisted by silver surface plasmonic splitter," Opt. Express **25** (2017) 19129 (DOI: 10.1364/OE.25.019129).
[9] S. Fan, *et al.*: "Comment on "Nonreciprocal light propagation in a silicon photonic circuit"," Science **335** (2012) 38 (DOI: 10.1126/science.1216682).
[10] L. Feng, *et al.*: "Response to comment on "Nonreciprocal light propagation in a silicon photonic circuit"," Science **335** (2012) 38 (DOI: 10.1126/science.1213954).
[11] D. K. Gramotnev, *et al.*: "Plasmonics beyond the diffraction limit," Nature Photin. **4** (2010) 83 (DOI: 10.1038/nphoton.2009.282).
[12] A. Hosseini, *et al.*: "Nanoscale surface plasmon based resonator using rectangular geometry," Appl. Phys. Lett. **90** (2007) 181102 (DOI: 10.1063/1.2734380).
[13] A. Pannipitiya, *et al.*: "Improved transmission model for metal-dielectric-metal plasmonic waveguides with stub structure," Opt. Express **18** (2010) 6191 (DOI: 10.1364/OE.18.006191).
[14] P. Chen, *et al.*: "Plasmonic filters and optical directional couplers based on wide metal-insulator-metal structure," Opt. Express **19** (2011) 7633 (DOI: 10.1364/OE.19.007633).
[15] S. Sederberg, *et al.*: "Ultrafast all-optical switching in a silicon-based plasmonic nanoring resonator," Opt. Express **19** (2011) 23494 (DOI: 10.1364/OE.19.023494).
[16] Z. Han, *et al.*: "Plasmon-induced transparency with detuned ultra-compact Fabry-Perot resonators in integrated plasmonic devices," Opt. Express **19** (2011) 3251 (DOI: 10.1364/OE.19.003251).
[17] M. Komatsu, *et al.*: "Compact polarization rotator based on surface plasmon polariton with low insertion loss," IEEE Photon. J. **4** (2012) 707 (DOI: 10.1109/JPHOT.2012.2195650).
[18] J. N. Caspers, *et al.*: "Experimental demonstration of an integrated hybrid plasmonic polarization rotator," Opt. Lett. **38** (2013) 4054 (DOI: 10.1364/OL.38.004054).
[19] Y.-J. Chang, *et al.*: "Photonic-quasi-TE-to-hybrid-plasmonic-TM polarization mode converter," J. Lightw. Technol. **33** (2015) 4261 (DOI: 10.1109/JLT.2015.2464685).
[20] Y.-J. Chang, *et al.*: "Embedded-silicon-strip-to-hybrid-plasmonic waveguide polarization mode converter," IEEE Photon. Technol. Lett. **29** (2017) 759 (DOI: 10.1109/LPT.2017.2684182).
[21] K. Wen, *et al.*: "Theoretical analysis of plasmonic unidirectional propagation at visible frequency based on subwavelength waveguide," Opt. Commun. **336** (2015) 243 (DOI: 10.1016/j.optcom.2014.10.015).
[22] J. S. Jensen, *et al.*: "Systematic design of photonic crystal structures using topology optimization: Low-loss waveguide bends," Appl. Phys. Lett. **84** (2004) 2022 (DOI: 10.1063/1.1688450).
[23] Y. Tsuji, *et al.*: "Design of optical circuit devices based on topology optimization," IEEE Photon. Technol. Lett. **18** (2006) 850 (DOI: 10.1109/LPT.2006.871686).
[24] L. H. Frandsen, *et al.*: "Topology optimized mode conversion in a photonic crystal waveguide fabricated in silicon-on-insulator material," Opt. Express **22** (2014) 8525 (DOI: 10.1364/OE.22.008525).
[25] Z. Zhang, *et al.*: "Design of ultra-compact triplexer with function-expansion based topology optimization," Opt. Express **23** (2015) 3937 (DOI: 10.1364/OE.23.003937).
[26] A. Iguchi, *et al.*: "Efficient topology optimization of optical waveguide devices utilizing semi-vectorial finite-difference beam propagation method," Opt. Express **25** (2017) 28210 (DOI: 10.1364/OE.25.028210).
[27] A. Iguchi, *et al.*: "Topology optimal design for optical waveguides using time domain beam propagation method," IEICE Electron. Express **15** (2018) 20180417 (DOI: 10.1587/elex.15.20180417).
[28] A. Koda, *et al.*: "A study on topology optimization of plasmonic waveguide devices using function expansion method and evolutionary approach," J. Lightw. Technol. **37** (2019) 981 (DOI: 10.1109/JLT.2018.2884903).
[29] R. Storn and K. Price: "Differential Evolution - A simple and efficient adaptive scheme for global optimization over continuous spaces," J. Glob. Optim. **11** (1997) 341 (DOI: 10.1023/A:1008202821328).
[30] A. D. Rakić, *et al.*: "Optical properties of metallic films for vertical-cavity optoelectronic devices," Appl. Opt. **37** (1998) 5271 (DOI: 10.1364/AO.37.005271).
[31] Y. Tsuji, *et al.*: "Finite element method using port truncation by perfectly matched layer boundary conditions for optical waveguide discontinuity problems," J. Lightw. Technol. **20** (2002) 463 (DOI: 10.1109/50.988995).